



CENTER FOR INFRASTRUCTURE ENGINEERING STUDIES

**Determination of Shear-wave Velocity Profiles from
Surface (Rayleigh) Seismic Waves: Wahite Ditch and St.
Francis River Bridge Sites, Southeast Missouri**

By

Dr. Neil Anderson

Dr. Genda Chen

Dr. Ronaldo Luna

S. Kociu

T. Thitimakorn

University Transportation Center Program at

The University of Missouri-Rolla

**UTC
R72**

Disclaimer

The contents of this report reflect the views of the author(s), who are responsible for the facts and the accuracy of information presented herein. This document is disseminated under the sponsorship of the Department of Transportation, University Transportation Centers Program and the Center for Infrastructure Engineering Studies UTC program at the University of Missouri - Rolla, in the interest of information exchange. The U.S. Government and Center for Infrastructure Engineering Studies assumes no liability for the contents or use thereof.

Technical Report Documentation Page

1. Report No. UTC R72	2. Government Accession No.	3. Recipient's Catalog No.	
4. Title and Subtitle Determination of Shear-wave Velocity Profiles from Surface (Rayleigh) Seismic Waves: Wahite Ditch and St. Francis River Bridge Sites, Southeast Missouri		5. Report Date June 2003	
		6. Performing Organization Code	
7. Author/s Dr. Neil Anderson, Dr. Genda Chen, Dr. Ronaldo Luna, S. Kociu, T. Thitimakorn		8. Performing Organization Report No. RG001159	
9. Performing Organization Name and Address Center for Infrastructure Engineering Studies/UTC program University of Missouri - Rolla 223 Engineering Research Lab Rolla, MO 65409		10. Work Unit No. (TRAIS)	
		11. Contract or Grant No. DTRS98-G-0021	
12. Sponsoring Organization Name and Address U.S. Department of Transportation Research and Special Programs Administration 400 7 th Street, SW Washington, DC 20590-0001		13. Type of Report and Period Covered Final	
		14. Sponsoring Agency Code	
15. Supplementary Notes			
16. Abstract UMR will acquire multi-channel surface-wave (Rayleigh wave) seismic data in the vicinity of the Wahite Ditch Bridge and St. Francis River Bridge test sites. These Rayleigh wave data will be processed and analyzed, and used to construct subsurface shear-wave velocity profiles to depths on the order of 100 feet. These Rayleigh wave data will be compared to borehole seismic and seismic CPT data previously acquired at the test sites. The objective is to determine if the multi-channel surface-wave seismic tool is a cost-effective and accurate means of determining shear-wave velocity profiles for the shallow subsurface.			
17. Key Words Non-destructive imaging, technology transfer, Rayleigh waves, shears waves.	18. Distribution Statement No restrictions. This document is available to the public through the National Technical Information Service, Springfield, Virginia 22161.		
19. Security Classification (of this report) unclassified	20. Security Classification (of this page) unclassified	21. No. Of Pages	22. Price

EXECUTIVE SUMMARY

Researchers from the University of Missouri-Rolla (UMR) and their scientific research colleagues from the Mining Institute in Perm (MIP), Russia, acquired multi-channel surface-wave (Rayleigh wave) seismic control at six separate bridge sites in southeast Missouri. Each acquired surface wave data set was processed (spectral analysis of surface waves; SASW) and transformed into a site-specific vertical shear-wave velocity profile (SASW shear-wave velocity profile). Each SASW shear-wave velocity profile extends from the surface to a depth on the order of 60 m.

The SASW shear-wave velocity profiles generated for each bridge site were compared to other geotechnical data (provided by the Missouri Department of Transportation; MoDOT), including seismic cone penetrometer test shear-wave velocity profiles (SCPT shear-wave velocity profiles), cross-borehole shear-wave velocity profiles (CH shear-wave velocity profiles), and borehole lithology logs. The primary objective of this study was to determine how well SASW shear-wave velocity profiles compare to more standard geotechnical data.

The geotechnical data presented herein indicate the SASW shear-wave velocity profiles correlate as well with subsurface lithology logs and available cross-borehole shear-wave velocity control. More specifically, clays, silts and sands exhibit relatively characteristic SASW-velocities, which increase almost monotonically (step-wise and incrementally) with increasing depth of burial. We believe these correlations demonstrate that SASW shear-wave velocities are reliable.

The data presented herein indicate the SCPT shear-wave profiles do not appear to correlate well with available borehole lithologic control, available cross-borehole shear-wave velocity profiles, or the generated SASW shear-wave velocity profiles. SCPT shear-wave interval velocities often vary significantly over short vertical distances within essentially uniform lithologic units. Additionally, SCPT shear-wave velocities for essentially the same lithologic units differ significantly at proximal test sites. In our opinion, the SCPT shear-wave interval velocity data (as provided by MoDOT) cannot be used to assess the reliability/reasonableness of the SASW shear-wave velocity profiles.

On the basis of this study, we conclude that SASW shear-wave velocity profiles are reliable. In our opinion, the SASW technique can be used to estimate the engineering properties of soil.

We recommend an expanded SASW study. We recommend the acquisition of SASW, SCPT, cross-borehole seismic and SPT data at multiple additional test sites in Missouri, in an effort to determine inter-relationships in a statistically meaningful way. We also recommend the acquisition of SASW data at select sites in Missouri, in an effort to assess the utility of this tool in terms of determining depth to bedrock, estimating the engineering properties of bedrock, and identifying heterogeneities (e.g. karstic cavities) within bedrock. Further, we recommend the acquisition of SASW data across paved roadways in order to assess the capabilities of this tool in terms of estimating asphalt and pavement thicknesses, and sub-grade conditions.

ACKNOWLEDGEMENTS

The principal investigators would like to thank Mr. Tom Fennessey, PE, Missouri Department of Transportation, for his support, encouragement and direction. Mr. Kevin McLain, PE, Missouri Department of Transportation, generated the SCPT data and provided copies of the same.

We would also like to extend our appreciation to the geophysics field crew, including graduate students, A. Akingbade, P. Bytirin, J. Baranov, R. Dyagilev, and A. Ismail. Technical support was provided by Mr. Oleg Kovin.

TABLE OF CONTENTS

	Page #
TITLE PAGE	i
TECHNICAL REPORT DOCUMENTATION PAGE	ii
EXECUTIVE SUMMARY	iii
ACKNOWLEDGEMENTS	iv
TABLE OF CONTENTS	v
LIST OF ILLUSTRATIONS	vii
1. INTRODUCTION	1
2. STATEMENT OF PROBLEM/SCOPE OF WORK	1
Overview of Seismic Cone Penetrometer (SCPT) Technique	1
Overview of Cross-Borehole (CH) Shear-Wave Surveying	2
Summary	3
3. OBJECTIVE	3
4. INDUCED SEISMIC WAVES	3
5. RAYLEIGH WAVES (OVERVIEW OF SASW TECHNIQUE)	5
6. SASW FIELD TECHNIQUE	6
7. PROCESSING OF SASW DATA	6
8. SASW SHEAR-WAVE VELOCITY PROFILES: CONSIDERATIONS	7
9. FIELD SITES: LOCATIONS AND GEOTECHNICAL DATA	7
A-3709 Bridge Site #1	8
A-5648 Bridge Site #2	8
L-472 Bridge Site #3	8
A-1466 Bridge Site #4	8
L-302 Bridge Site #5	8
A-5460 Bridge Site #6	8
10. PRESENTATION OF SASW AND SCPT SEISMIC DATA	8
A-3709 Bridge Site #1	8
A-5648 Bridge Site #2	9
L-472 Bridge Site #3	10
A-1466 Bridge Site #4	10
L-302 Bridge Site #5	11
A-5460 Bridge Site #6	12

11. COMPARISON OF SASW AND SCPT VERTICAL SHEAR-WAVE PROFILES	12
12. CONCLUSIONS AND RECOMMENDATIONS	13
13. SUGGESTED REFERENCES	14

LIST OF ILLUSTRATIONS

	Page #
Figure 1: Particle motions associated with compressional waves (P-waves; upper caption) and shear waves (S-waves; lower caption).	4
Figure 2: Particle motions associated with Rayleigh waves (upper caption) and Love waves (lower caption).	4
Figure 3: SASW receiver array configuration.	6
Figure 4: Map of southeast Missouri showing locations of Bridge Sites #1 through #6. Δ denotes SASW test site. (Site #1: A-3709 Bridge; Site #2: A-5648 Bridge; Site #3: L-472 Bridge; Site #4: A-1466 Bridge; Site #5: L-302 Bridge; Site #6: A-5460 Bridge.)	15
Figure 5: A-3709 Bridge Site #1 (Figure 4).	16
Figure 6: A-5648 Bridge Site #2 (Figure 4).	17
Figure 7: L-472 Bridge Site #3 (Figure 4).	18
Figure 8: A-1446 Bridge Site #4 (Figure 4).	19
Figure 9: L-302 Bridge Site #5 (Figure 4).	20
Figure 10: A-5460 Bridge Site #6 (Figure 4).	21
Figure 11: Shear-wave velocity profiles for A-3709 Bridge Site #1 (Figures 4 and 5).	22
Figure 12: Shear-wave velocity profiles for A-5648 Bridge Site #2 (Figures 4 and 6).	23
Figure 13: Shear-wave velocity profiles for L-472 Bridge Site #3 (Figures 4 and 7).	24
Figure 14: Shear-wave velocity profiles for A-1446 Bridge Site #4 (Figures 4 and 8).	25
Figure 15: Shear-wave velocity profile for L-302 Bridge Site #5 (Figures 4 and 9).	26
Figure 16: Shear-wave velocity profile for A-5460 Bridge Site #6 (Figures 4 and 10).	27

1. INTRODUCTION

In May 2002, researchers from the University of Missouri-Rolla (UMR) and scientific colleagues from the Mining Institute in Perm (MIP), Russia, acquired multi-channel surface-wave (Rayleigh wave) seismic control at six separate bridge sites in southeast Missouri. Each acquired surface wave data set was processed (including spectral analyses; SASW) and transformed into a site-specific vertical shear-wave velocity profile with maximum depths in excess of 60 m. Herein, these SASW shear-wave velocity profiles are presented and compared to other geotechnical data provided by the Missouri Department of Transportation (MoDOT) including seismic cone penetrometer test (SCPT) derived shear-wave profiles, cross-borehole (CH) shear-wave profiles and borehole lithologic control. In section 12 of this report, recommendations for further SASW investigative studies are presented.

This SASW project is consistent with MoDOT's Research Focus Plan wherein the evaluation of recently-developed surface (Rayleigh) wave technology was identified as a priority for the Geotechnical RDT TAG during the MOTREC/MoDOT biennial meeting (8/7/01).

2. STATEMENT OF PROBLEM/SCOPE OF WORK

The determination or estimation of the in-situ shear modulus of shallow, unconsolidated, non-cohesive soils at bridge sites is critically important in terms of the evaluation of foundation integrity. This is particularly true in terms of assessing the soil's response to strong ground motion.

Historically, MoDOT engineers have estimated the shear modulus of non-cohesive soils on the basis of standard penetration tests (SPT) and laboratory strain tests. More recently, MoDOT has estimated shear modulus on the basis of seismic cone penetrometer tests (SCPT) and, at least on an experimental basis, on the basis of cross-borehole (CH) shear-wave seismic velocities. As noted in the following text, these latter two test procedures (SCPT and CH) have their own characteristic strengths and weaknesses.

Overview of Seismic Cone Penetrometer Test (SCPT) Technique: As utilized by MoDOT, this technique employs a downhole shear-wave geophone (acoustic receiver coupled to the tip of the SCPT cone) and a surface hammer shear-wave source. As the SCPT cone is pressed into the soil, it is halted momentarily at predetermined incremental depths (the center-to-center spacing of these "unit layers" is generally on the order of 1 m) and the surface shear-wave source is discharged twice – with opposite directional impacts - thereby generating two opposite-polarity shear-wave records.

The arrival time of the shear-wave energy (travel time from source to geophone) is measured at the top of each layer (T_{n_top}) and at the base of each layer (T_{n_base}). The average shear-wave interval velocity (β_{n_int}) for the nth layer is then calculated as:

$$\beta_{n_int} = \Delta Z_n / \Delta T_n \quad \text{Equation 1}$$

where:

β_{n_int} = shear wave interval velocity for nth layer
 ΔZ_n = "acoustic" thickness of nth layer = $L_{n_top} - L_{n_base}$
 L_{n_top} = source-to-geophone separation at top of nth layer
 L_{n_base} = source-to-geophone separation at base of nth layer
 ΔT_n = transit time through nth layer = $T_{n_top} - T_{n_base}$
 T_{n_top} = travel time from hammer source to geophone at top of nth layer
 T_{n_base} = travel time from hammer source to geophone at base of nth layer

If the arrival times ($T_{n_{top}}$; $T_{n_{base}}$) of the shear wave energy at the top and base each layer are accurately determined and if the source-to-geophone separations are accurately measured, the SCPT tool is capable of providing accurate subsurface shear-wave interval velocities ($\beta_{n_{int}}$). However, if arrival times are not accurately determined, the output shear-wave interval velocities will be inaccurate. There are two most-probable causes of such error. First, it is conceivable that earlier arriving compressional-wave (P-wave) energy (upgoing and/or downgoing) could be misinterpreted as shear-wave energy, particularly at shallow receiver depths (where the P-wave and S-wave arrivals are almost superposed). A second possible cause of “error” is related to the accuracy with which shear-wave arrival times can be determined at each test depth. Even in those situations where shear-wave energy is clearly differentiated from earlier arriving compressional wave energy, there is some intrinsic uncertainty in the determination of shear-wave arrival times. Small errors (e.g. ± 1 ms) in estimated transit time (ΔT_n) through the nth layer will generate corresponding errors in the estimated shear-wave interval velocities ($\beta_{n_{int}}$) assigned to the nth layer. For example, if the transit time (ΔT_n) through a 1 m thick layer (with a shear-wave velocity of 250 m/s) is underestimated by 1 ms, the interval velocity ($\beta_{n_{int}}$) assigned to that layer will be overestimated by 33%.

If the interval shear-wave velocity ($\beta_{n_{int}}$) assigned to the nth layer is inaccurate (i.e., too high or too low, as discussed above), the shear-wave interval velocity ($\beta_{n+1_{int}}$) assigned to the underlying layer (n+1th) layer will also be inaccurate (i.e., too low or too high, respectively; assuming of course that arrival times of shear-wave energy is correctly determined for n+1th layer).

Inaccurate determinations of the source-to-geophone separations ($L_{n_{top}}$, $L_{n_{base}}$) will similarly result in inaccurate shear-wave interval velocity estimates ($\beta_{n_{int}}$).

In terms of overall utility, the SCPT tool works well in clays, silts and sands – but doesn’t work well in gravels (which can damage the cone head). Additionally, because of confining pressures, the SCPT tool is usually not capable of providing shear-wave velocity control at depths greater than 20 m (in Mississippi Embayment area). Lastly, the SCPT tool can access only those sites accessible to a drill rig.

Overview of Cross-Borehole (CH) Shear-Wave Surveying: As utilized by MoDOT-funded researchers, this technique employs twinned boreholes separated by surface distances on the order of 3-4 m (10-15 ft). (Subsurface separations are determined using a borehole inclinometer.) MoDOT test boreholes have been cased with capped PVC tubing, grouted and bailed.

The acquisition of CH shear-wave data is relatively straight forward. An arm-locking shear-wave hammer source is lowered to the base of one of the twinned boreholes and coupled to the PVC casing; an arm-locking triaxial geophone is lowered to the same depth in the adjacent hole and locked in place. The hammer source is discharged twice – with opposite directional impacts - thereby generating two opposite-polarity shear-wave records. The source and geophone are then raised to the top of the borehole at regular pre-determined intervals (corresponding to center of each “layer”; generally on the order of 1 m). At each pre-determined depth location, the tools are locked in place and the source is discharged twice. After field work is completed, the interpreters analyze the acquired data and calculate interval shear-wave velocities (β_{int} ; $\Delta x/\Delta t$) for each layer tested on the basis of measured borehole separation (Δx) and shear-wave travel time (Δt ; measured arrival time of first shear-wave energy).

The cross-borehole shear-wave technique is capable of providing accurate in-situ, shear-wave interval velocities in unconsolidated sediment. These shear-wave interval velocities however, at least in theory, may not be as accurate as the corresponding SCPT shear-wave interval velocities. The reason is that the shear-wave velocities of thin low-velocity layers will tend to be overestimated because the shear-wave energy that arrives “first” at the relevant receiver will tend to be a refraction from an adjacent higher-velocity layer (rather than the desired direct arrival).

The biggest shortcomings of the cross-borehole shear-wave technique are related to overall cost and site accessibility, as twinned boreholes are required. On the upside, the tool can be used to determine shear-wave velocities at depths in excess of 60 m.

Summary: As noted in the preceding text, the conventional tools used to estimate the shear moduli of soils have their own characteristic strengths and weaknesses. Some techniques are more expensive, some provide for greater depth of investigation, some don't work well in larger-grained sediment, etc. Suffice to say – none of the conventional tools currently employed by MoDOT is suitable for all site investigations.

In an attempt to evaluate an alternate, recently-developed methodology that could prove to be more effective than conventional techniques at certain sites, MoDOT asked UMR researchers to acquire surface wave (Rayleigh wave) seismic data at six bridge sites in southeast Missouri. These surface-wave data were processed (essentially inverted) and transformed into vertical shear-wave velocity profiles (SASW shear-wave velocity profiles). In theory, the shear-wave data generated from the “spectral analysis of surface waves” (SASW) technique are reliable and can be used to estimate the shear moduli of the soil.

3. OBJECTIVE

The objective of this study was to acquire Rayleigh (surface) wave data at six bridge sites in southeast Missouri using both active and passive sources, and an orthogonal array of paired low-frequency geophones. The intent was to process (spectral inversion; SASW) these Rayleigh wave data, and generate a shear-wave velocity profile for each site (to depths on the order of 60 m). These shear-wave velocity profiles were to be compared with other geotechnical data acquired at each site (including SCPT shear-wave velocity profiles, CH shear-wave velocity profiles, and lithologic control).

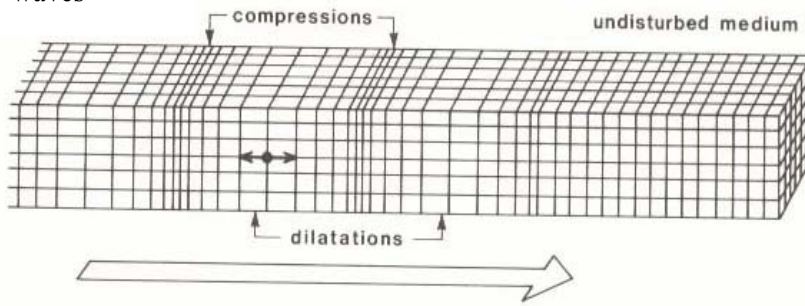
4. INDUCED SEISMIC WAVES

When an acoustic source (weight drop, dynamite charge, etc.) is discharged at or near the surface of the earth, two fundamental types of acoustic waves (strain energy) are produced: body waves and surface waves. Two types of body waves can propagate through an elastic solid (compressional waves and shear waves). Similarly, two types of surface waves can propagate along the earth's surface (Rayleigh waves and Love waves).

Compressional waves (or P-waves) propagate by compressional and dilatational strains in the direction of wave travel (Figure 1). Particle motion involves oscillation, about a fixed point, in the direction of wave propagation. Shear waves (or S-waves) propagate by a pure strain in a direction perpendicular to the direction of wave travel (Figure 1). Body waves are essentially non-dispersive over the range of frequencies employed for earthquake studies and seismic exploration (i.e., all component frequencies propagate at the same velocity). The propagation velocities of body waves are a function of the engineering properties of the medium through which they are traveling (Figure 1).

Love waves propagate along the surface of a layered solid (earth's surface) if the shear-wave velocity of the uppermost layer is lower than that of the underlying layer (e.g., unconsolidated strata overlying bedrock). Love waves are polarized shear waves with an oscillatory particle motion parallel to the free surface and perpendicular to the direction of wave motion (Figure 2). Love waves are dispersive, and are characterized by velocities between the shear-wave velocity of the shallowest layer and that of deeper layers. The amplitude of a Love wave decreases exponentially with depth. The lower component frequencies of Love waves involve particle motion at greater depth and therefore generally exhibit higher velocities.

(a) P-waves



$$\alpha = [(K + 4\mu/3)/\rho]^{1/2}$$

$$\beta = [\mu/\rho]^{1/2}$$

where:

α = P-wave velocity (V_p)

β = S-wave velocity (V_s)

K = bulk modulus

μ = shear modulus

ρ = density

(b) S-waves

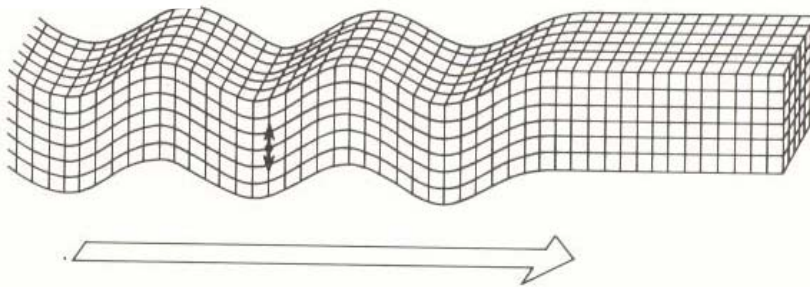
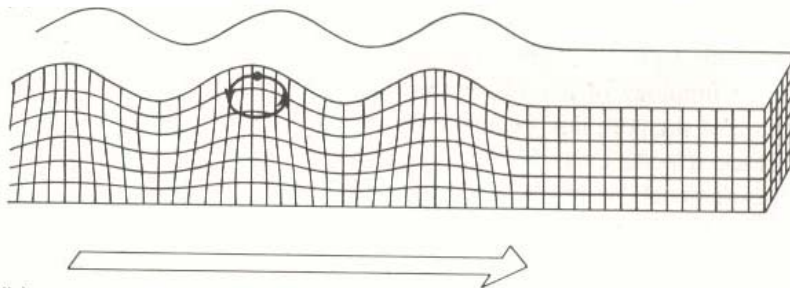


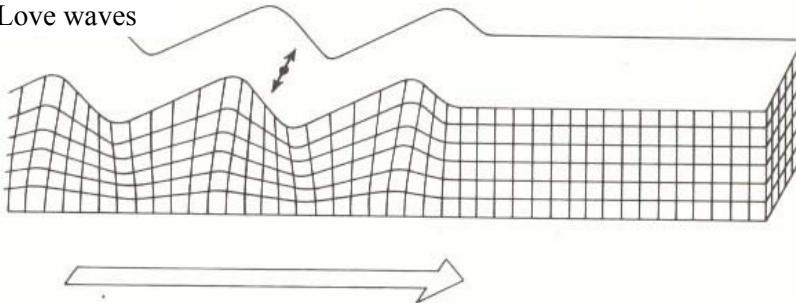
Figure 1: Particle motions associated with compressional waves (P-waves; upper caption) and shear waves (S-waves; lower caption).

(a) Rayleigh waves



- Rayleigh wave particle motion
- retrograde elliptical
- decreases exponentially with depth
- function of α and β

(b) Love waves



- Love wave particle motion
- horizontal
- decreases exponentially with depth
- function of β

Figure 2: Particle motions associated with Rayleigh waves (upper caption) and Love waves (lower caption).

Rayleigh waves propagate along the earth's surface (free surface). The associated particle motion is elliptical in a plane perpendicular to the surface and containing the direction of propagation (Figure 2). The orbital motion is in the opposite sense to the circular motion associated with a water wave, and is often described as retrograde elliptical. The amplitude of a Rayleigh wave decreases exponentially with depth (Figure 2). Progressively lower frequency components of Rayleigh waves involve particle motion over progressively greater depth ranges (relative to free surface). Rayleigh waves in a heterogeneous medium (with respect to velocity) are therefore dispersive. The velocities with which the highest component frequencies travel are a function of the engineering properties of the shallowest sediment. The velocities with which progressively lower frequencies travel are functions of the varying engineering properties over a progressively greater range of sediment depths. In the "spectral analysis of surface wave" (SASW) technique, the phase velocities of the component frequencies are calculated. These data are then inverted and used to generate a vertical shear-wave velocity profile.

5. RAYLEIGH WAVES (OVERVIEW OF SASW TECHNIQUE)

Rayleigh waves propagate along the free surface of the earth, with particle motions that decay exponentially with depth (Figure 2). The lower component frequencies of Rayleigh waves involve particle motion at greater depths. In a homogeneous (non-dispersive) medium, Rayleigh wave phase velocities are constant can be determined using the following equation:

$$V_R^6 - 8\beta^2 V_R^4 + (24 - 16\beta^2/\alpha^2)\beta^4 V_R^2 + 16(\beta^2/\alpha^2 - 1)\beta^6 = 0 \quad \text{Equation 2}$$

where:

- V_R is the Rayleigh wave velocity within the uniform medium
- β is the shear-wave velocity within the uniform medium (also denoted V_s)
- α is the compressional wave velocity within the uniform medium (also denoted V_p)

Rayleigh wave velocities, as noted in Equation 1, are a function of both the shear-wave velocity and compressional wave velocity of the subsurface.

In a heterogeneous earth, shear-wave and compressional-wave velocities vary with depth. Hence, the different component frequencies of Rayleigh waves (involving particle motion over different depth ranges) exhibit different phase velocities (Bullen, 1963). The phase velocity of each component frequency being a function of the variable body wave velocities over the vertical depth range associated with that specific wavelength. More specifically, in a layered earth, the Rayleigh wave phase velocity equation has the following form:

$$V_{Rj}(f_j, C_{Rj}, \beta, \alpha, \rho, h) = 0 \quad (j = 1, 2, \dots, m) \quad \text{Equation 3}$$

where:

- f_j is the frequency in Hz
- V_{Rj} is the Rayleigh-wave phase velocity at frequency f_j
- $\beta = (\beta_1, \beta_2, \dots, \beta_n)^T$ is the s-wave velocity vector
- β_i is the shear-wave velocity of the i th layer
- $\alpha = (\alpha_1, \alpha_2, \dots, \alpha_n)^T$ is the compressional p-wave velocity vector
- α_i is the P-wave velocity of the i th layer
- $\rho = (\rho_1, \rho_2, \dots, \rho_n)^T$ is the density vector
- ρ_i is the density of the i th layer

$\mathbf{h} = (\mathbf{h}_1, \mathbf{h}_2, \dots, \mathbf{h}_{n-1})^T$ is the thickness vector
 \mathbf{h}_i the thickness of the i th layer
 n is the number of layers within the earth model

The spectral analysis of surface waves (SASW) technique is based on the relationship between Rayleigh wave phase velocities and the depth-range of associated particle motion. More specifically, in this technique, phase velocities are calculated for each component frequency of field-recorded Rayleigh waves (active and passive monitoring). The resultant dispersion curve (phase velocity vs. frequency) is then inverted using a least-squares approach and a vertical shear-wave velocity profile is generated (Miller *et al.*, 2000; Nazarian *et al.*, 1983; Stokoe *et al.*, 1994; Park *et al.*, 2001; Xia *et al.*, 1999).

6. SASW FIELD TECHNIQUE

The acquisition of the “active” higher frequency (8-20 Hz) Rayleigh wave data was relatively straightforward. At each bridge site, active Rayleigh wave data were generated using both a truck-mounted Bison EWG weight drop source and a sledge hammer source. The weight drop generated higher amplitude Rayleigh waves and was employed when the source was more than 200 feet from the nearest receiver (Figure 3). The sledge hammer generated lower amplitude Rayleigh waves and was employed when the source was less than 200 feet from the nearest receiver or in areas inaccessible to the truck-mounted weight drop. The Rayleigh waves generated at each source location were recorded by one or two pairs of in-line low-frequency receivers (geophones) centered about a specific (designated) target location (Figure 3). The spacing between each receiver pair was increased for longer source-receiver offsets and decreased for shorter source-receiver offsets. Multiple Rayleigh wave records were generated and stacked for each source-receiver array, in an effort to increase signal-to-noise ratios. Background noise was mostly associated with vehicular traffic, which at some sites was relatively heavy.

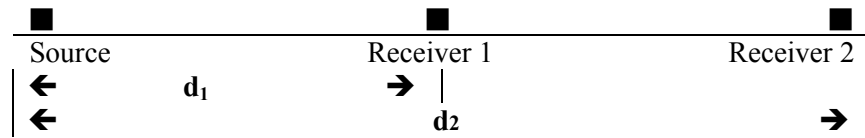


Figure 3: SASW receiver array configuration.

The Rayleigh waves generated from the “active” impulsive sources generated relatively high-frequency signal (8-20 Hz range). Low-frequency (2-12 Hz) surface wave phase velocities were determined from the analysis of microseismic noise recorded during passive monitoring. During processing, these two dispersion curves (8-20 Hz and 2-12 Hz) were combined to form one representative curve over the entire range of frequencies (2-20 Hz).

7. PROCESSING OF SASW DATA

The Rayleigh waves recorded during both “active” and “passive” monitoring were transformed from the time domain into the frequency domain using Fast Fourier Transform (FFT) techniques. For each component frequency, the corresponding phase difference ($\Theta(\mathbf{f})$) between each receiver pair was computed. The travel time (Δt) between receivers was calculated using the equation:

$$\Delta t(\mathbf{f}) = \Theta(\mathbf{f})/2\pi\mathbf{f} \quad \text{Equation 4}$$

Since the distance between each pair of receivers ($\Delta d = d_2 - d_1$; Figure 3) was known, the Rayleigh wave phase velocity corresponding to each component frequency (f) was calculated using the following formula:

$$V_R(f) = \Delta d / \Delta t(f) \quad \text{Equation 5}$$

The corresponding wavelengths (λ_R) were calculated as follows:

$$\lambda_R(f) = V_R(f) / f \quad \text{Equation 6}$$

These field-based data were used to generate site-specific dispersion curves ($V_R(f)$ versus $\lambda_R(f)$) for each receiver pair mid-point at each bridge site. The site-specific dispersion curves (**DCS**) generated from field-acquired Rayleigh wave data were then transformed into vertical shear-wave velocity profiles (**SASW** shear-wave velocity profile). Transformations were based on the following assumptions: 1) α/β decreased from 3.0 (for shallowest layers) to 1.71 (for deepest layers), and 2) density (ρ) = $1.64 + 0.0008 * \beta$ (where α is the compressional-wave velocity in m/s and β is shear-wave velocity in m/s).

The process through which the field-determined dispersion curves (**DCS**) were transformed into vertical shear-wave velocity profiles was iterative and approximate. In this procedure, an initial “theoretical 1-D vertical shear-wave model” (profile N_1) was created for each bridge site. This initial “best-guess” model (N_1) was used to generate an initial “theoretical dispersion curve” (**DC₁**). The theoretical dispersion curve (**DC₁**) was then compared to the corresponding site-specific dispersion curve (**DCS**). Differences between the **DC₁** and **DCS** curves were noted, and the N_1 profile was changed accordingly. The output of this process was an N_2 profile. The N_2 profile was then used to generate a new theoretical dispersion curve (**DC₂**). Differences between the **DC₂** and **DCS** curves were noted, and the N_2 profile was changed accordingly. This process was repeated iteratively, until convergence was obtained.

8. SASW SHEAR-WAVE PROFILES: CONSIDERATIONS

Consideration A: Rayleigh-wave phase velocities were determined using paired sets of receivers separated by distances on the order of tens of feet. The Rayleigh-wave phase velocities therefore represent “average” subsurface velocities determined over the breadth and depth of the corresponding receiver-receiver interval. Thus, the vertical shear-wave velocity profiles also represent “average” subsurface velocities.

Consideration B: Rayleigh-wave data were acquired in a “noisy” environment (at some sites, vehicular traffic noise was intense). Background noise contaminated the “passive” Rayleigh wave data in particular, and made the determination of shear-wave velocities at increasing depths less accurate.

Consideration C: Shear-wave velocities are determined sequentially (from shallowest horizon to deepest horizon). Thus any inaccuracies (with respect to the determination of shallow velocities) produce cascading errors. The result is that the accuracy of the shear-wave estimates tends to diminish with increasing depth.

9. FIELD SITES: LOCATIONS AND GEOTECHNICAL DATA

SASW, SCPT and lithologic data were acquired at six different bridge sites (Sites #1 - #6; Figure 4) in southeast Missouri. The SASW data were acquired using orthogonal arrays of paired geophones. The SCPT data acquired at test locations near the center of the SASW arrays are referred to as XCPT data.

A-3709 Bridge Site #1: Surface-wave (SASW) data were acquired in the median lane (twinned dual lane highway), immediately to the west of the St. Francis River bridges (Figures 4 and 5). The SASW paired-geophone array was centered about the XCPT test location, about 30 m to the west of the MoDOT B-1 borehole. SASW active source locations were offset farther to the west (in the median lane and in-line with the SASW geophones). Additional SCPT shear-wave seismic (C2) and boring log (B2) data were acquired along the embankment immediately to the south of the east-bound lane. The C2/B2 sites are about 50 m to the southeast of the center of the SASW paired geophone array (Figure 5).

A-5648 Bridge Site #2: SASW data were acquired in the median lane (twinned dual lane roadways), immediately to the west of the Wahite Ditch bridges (Figures 4 and 6). The SASW paired-geophone array was centered about the XCPT test location, about 30 m to the west of the twinned B1 boreholes and corresponding C1 SCPT site. SASW active source locations were offset farther to the west (in the median lane and in-line with paired geophones). The A-5648 bridge cross-borehole shear-wave data were acquired at the twinned B1 borehole locations.

L-472 Bridge Site #3: SASW data were acquired to the southwest of the existing bridges in the median lane of the twinned dual lane roadway (Figures 4 and 7). The SASW paired-geophone array was centered about the XCPT location, about 30 m to the southwest of the B1 borehole (also in median lane but nearer to crest of embankment). SASW source locations were offset to the southwest of the SASW geophone array (in median lane and in-line with geophone array).

A-1466 Bridge Site #4: SASW data were acquired in the median lane (twinned dual lane roadways), to the northeast of the existing bridges (Figures 4 and 8). The geophones were centered about the XCPT location (on inclined embankment), about 30 m to the northeast of the B2 borehole. The SASW source locations were offset farther to the northeast (in median lane and in-line with geophone array). The A-5648 bridge cross-borehole shear-wave data were acquired at the twinned B4/B5 borehole locations. The B4/B5 boreholes (separated by 15 ft) were located beneath the overpass, at the base of the embankment.

L-302 Bridge Site #5: SASW data were acquired along the levee immediately to the southwest of the existing two-lane bridge (Figures 4 and 9). The geophones were centered on the L-302 XCPT site, about 60 m from the bridge; the SASW source locations were in-line and offset further to the south along the levee. The closest borehole lithologic control was acquired at STA 133+58 (immediately to the southwest of the existing bridge).

A-5460 Bridge Site #6: SASW data were acquired along levee immediately to the southwest of the existing two-lane bridge (Figures 4 and 10). The geophones were centered on the A-5460 XCPT site (about 30 m from edge of stream; offsetting STA 180); the source locations were in-line and offset to the south away from the levee. The closest lithologic log was acquired at STA 180+33 (on south bank of stream).

10. PRESENTATION OF SASW AND SCPT SEISMIC DATA

A-3709 Bridge Site #1: The SASW vertical shear-wave profile from the A-3709 Bridge Site is shown in Figure 11. On the basis of average interval shear-wave velocity, the SASW profile can be divided into five units: Unit 1 (~0-3 m; ~140 m/s); Unit 2 (~3-14 m; ~220 m/s); Unit 3 (~14-42 m; ~280 m/s); Unit 4 (~42-54 m; 430-560 m/s); and Unit 5 (54+ m; >630 m/s).

Unit 1 (as per B-1 boring log; Figure 5) corresponds with a zone comprised mostly of silty clay (~0-3 m) *which is not described as stiff*; Unit 2 correlates with a zone comprised of predominantly clayey silt to brown silty sand (~3-10 m); Unit 3 correlates with a zone comprised mostly of fine to medium grained, dense gray sand (~10-46 m); Unit 4 (~46-54 m) correlates with a zone comprised mostly of medium

grained, very dense gray sand; and Unit 5 correlates with a zone described as cobbles and boulders (~54 m to base of logged borehole at about 58 m). Analysis of these data indicates there is a reasonable correlation between SASW shear-wave velocities and subsurface lithologies.

The XCPT shear-wave velocity profile (Figure 5) does not correlate quite so well with B1 lithologic data. More specifically, Unit 1 is characterized by shear-wave velocities ranging from 45 to 145 m/s, while Unit 2 is characterized by velocities ranging from 165 to 300 m/s.

The B2 boring log (Figures 5) can be divided into four units. Unit 1B (~0-1 m) is comprised of clay (*which is not described as stiff*). Unit 1C (~1-5 m) is comprised of *stiff to very stiff* clay. Unit 2 (~5-8 m) is described as predominantly sandy silt to silty sand; and Unit 3 (~8 m to base of log at 15 m) is described as predominantly gray medium sand. The C2 SCPT shear-wave velocity profile (Figure 11) correlates with these lithologic units in terms of “average lithologic unit velocities”, but exhibits significant standard deviation. More specifically, Unit 1B is characterized by a shear-wave interval velocity of ~30 m/s; Unit 1C is characterized by velocities ranging from ~210-340 m/s; Unit 2 is characterized by velocities ranging from ~140-260 m/s; and Unit 3 is characterized by velocities ranging from ~220-360 m/s.

As noted above, there appears to be a good correlation between SASW shear-wave velocities and subsurface lithology (as per the B1 boring log). More specifically, near-surface clays (*which are not described as stiff*) are characterized by SASW shear-wave velocities on the order of 140 m/s; clayey silt to brown silty sand is characterized by SASW shear-wave velocities on the order of 220 m/s; and fine-to-medium grained, dense gray sand is characterized by an SASW shear-wave velocity of about 280 m/s.

The SCPT shear-wave velocities, in contrast, do not appear to correlate particularly well with the subsurface lithology at the A-3709 bridge site. For example, while near-surface (<1 m depth) clay (*which is not described as stiff*) at the B2 site is characterized by SCPT shear-wave velocities on the order of 30 m/s, the other defined lithologic units are characterized by broad ranges in SCPT shear-wave velocities. More specifically, silty clays are characterized by SCPT shear-wave velocities ranging from ~45-145 m/s; stiff to very stiff clays are characterized by SCPT shear-wave velocities ranging from ~210-350 m/s; and clayey/sandy silts to silty sands are characterized by SCPT shear-wave velocities ranging from 140-300 m/s. The zone described as gray medium-grained sand is also characterized by a broad range in SCPT shear-wave velocities (~200-360 m/s).

The analysis of these data suggests the SCPT shear-wave velocity profiles and lithologic control at the A-3709 bridge site do not correlate well.

A-5648 Bridge Site #2: The SASW vertical shear-wave profile from the A-5648 Bridge Site is shown as Figure 12. On the basis of average estimated shear-wave velocity, the SASW profile can be divided into four units: Unit 1 (~0-6 m; ~130-170 m/s); Unit 2 (~6-18 m; ~230-270 m/s); Unit 3 (~18-48 m; ~270-350 m/s); and Unit 4 (~48+ m; >560 m/s).

Unit 1 (as per B1 boring log) corresponds with a zone comprised mostly of fat clay with sand (~0-6 m); Unit 2 correlates with a zone comprised mostly of interlayered fine to course-grained sands with scattered gravelly layers (~6-19 m); Unit 3 correlates with a fairly homogeneous zone comprised of mostly fine to course grained gray and tan sands (~19-49 m); Unit 4 (~49 m to base of logged borehole at ~60 m) correlates with a fairly homogeneous zone described as light gray and tan fine grained sand. These data indicate there is a direct correlation between SASW shear-wave velocities and subsurface lithologies.

The XCPT and C1 shear-wave velocity profiles (Figure 12) also correlate to some extent with these lithologic units. More specifically, Unit 1 is characterized by interval velocities that range from ~100-240 m/s; Unit 2 is characterized by a velocity of about 400 m/s.

As noted above, there appears to be a reasonable correlation between SASW shear-wave velocities and subsurface lithologies at the A-5648 Bridge Site. More specifically, near-surface clays (Unit 1) located away from the embankment are characterized by SASW shear-wave velocities ranging from about 130 to 170 m/s, with the deeper clays exhibiting progressively higher velocities. The underlying sands (Unit 2) are characterized by SASW shear-wave velocities ranging from about 230 to 270 m/s. Deeper sands (Units 3 and 4) exhibit increasingly higher velocities

The SCPT shear-wave velocities, in contrast, do not appear to correlate quite as well with the subsurface lithology at the A-5648 bridge site. For example, the non-compacted near-surface (<6 m depth) clays at the B2 site are characterized by SCPT shear-wave velocities ranging from 100-240 m/s, with the highest velocities being observed in the 2-3 m depth range. The underlying sands are characterized by SCPT shear-wave velocities on the order of 400 m/s. These values are significantly higher than the SASW shear-wave velocities corresponding to the same lithology/same depth.

The cross-borehole shear-wave velocity data acquired at the B1 site is also presented in Figure 12 (CH curve). These cross-borehole shear-wave seismic velocities correlate quite well with the SASW data. More specifically, the SASW shear-wave velocities from the surface to a depth of about 48 m are characterized by a velocity function that increases step-wise from an essentially about 130 m/s to 350 m/s. The same interval on the cross-borehole profile is characterized by shear-wave velocities that increase gradually from about 150 to 380 m/s. (Note: the cross-borehole data acquired at the A-5648 bridge site are excellent quality.)

L-472 Bridge Site #3: The SASW-generated vertical shear-wave profile from the L-472 Bridge Site is shown as Figure 13. On the basis of average estimated interval shear-wave velocity, the SASW profile can be divided into six units: Unit 1 (~0-4 m; ~90-110 m/s); Unit 2 (~4-10 m; ~140-160 m/s); Unit 3 (~10-14 m; ~190-210 m/s); Unit 4 (~14-22 m; ~230-260 m/s); Unit 5 (~22-60 m; ~310 m/s); and Unit 6 (>60 m; >400 m/s).

Unit 1 (as per B1 borehole lithology log) corresponds with a zone comprised mostly of silty clay (~0-4 m); Unit 2 correlates with a zone comprised of sandy silt to silty sand (~4-8 m); Unit 3 correlates with a zone comprised of mostly gray, medium dense to dense, medium to coarse sand (~8-14 m); Unit 4 correlates with a zone comprised mostly of gray, dense to very dense, medium to coarse sand (~14-22 m); Unit 5 consists mostly of gray, dense, fine sand (~22 m-base of borehole at ~25 m).

These SASW data and borehole data indicate there is a direct correlation between SASW shear-wave velocities and subsurface lithologies.

The SCPT shear-wave velocities (Figure 13) do not appear to correlate quite as well with subsurface lithology at the A-5648 bridge site. For example, the near-surface silty clays (<4 m depth) at the B1 site are characterized by XCPT shear-wave velocities ranging from ~115-145 m/s; the underlying sandy silts and silty sands are characterized by XCPT shear-wave velocities ranging from ~90-170 m/s. Note that the S2 shear-wave velocity profile differs significantly from the XCPT shear-wave velocity profile.

A-1466 Bridge Site #4: The SASW-generated vertical shear-wave profile from the A-1466 Bridge Site is shown as Figure 14. On the basis of average estimated interval shear-wave velocity, the SASW profile can be divided into six units: Unit 1 (~0-4 m; ~130-170 m/s); Unit 2 (~4-12 m; 190-230 m/s); Unit 3 (~12-43 m; ~250 m/s); Unit 4 (~43-48 m; ~370 m/s); and Unit 5 (>48 m; >460 m/s).

Unit 1 (as per B2 lithology log) corresponds with a zone comprised mostly of brown, sandy silt to silty sand (~0-4 m); Unit 2 correlates with a zone comprised of gray, stiff to very stiff, sandy silt to silty sand (~4-11 m); Unit 3 correlates with a zone comprised of mostly dense to very dense fine sand (~11 m to base of borehole at ~ 31 m).

These SASW data and borehole data indicate there is a reasonable correlation between SASW shear-wave velocities and subsurface lithologies.

The SCPT shear-wave velocities (Figure 14) also appear to correlate reasonably well with both subsurface lithology and SASW data. For example, the near-surface brown sandy silts and brown silty sands (<4 m depth) at the B2 site are characterized by XCPT shear-wave velocities ranging from ~160-200 m/s; the underlying stiff to very stiff sandy silts and silty sands are characterized by XCPT shear-wave velocities ranging from ~160-220 m/s. (Note that the XCPT and B1 shear-wave velocity profiles differ significantly.)

The cross-borehole shear-wave velocity data acquired at the B4/B5 location is also presented in Figure 14 (CH curve). These cross-borehole shear-wave seismic velocities correlate reasonably well with the SASW data. More specifically, the SASW curve is characterized by shear-wave velocities that increase step-wise from about 130 m/s to 350 m/s. The same interval on the CH profile is characterized by shear-wave velocities that increase gradationally (with minor irregularities) from about 150 to 380 m/s. (Note: the cross-borehole data acquired at the A-1446 bridge site range in quality from poor to good. The quality of these data was adversely affected by the high volume of traffic on I-55. As shown on the plan view map of Figure 8, the B4/B5 site is beneath and slightly to the east of the northbound A-1466 bridge. Ground level at the B4 location is about 10 m lower than at the XCPT location.)

L-302 Bridge Site #5: The SASW-generated vertical shear-wave profile from the L-302 Bridge Site is shown as Figure 15. On the basis of average estimated interval shear-wave velocity, the SASW profile can be divided into five units: Unit 1 (~0-6 m; ~120-140 m/s); Unit 2 (~6-10 m; ~160-180 m/s); Unit 3 (~10-18 m; ~180-260 m/s); Unit 4 (~18-48 m; ~280-320 m/s); and Unit 5 (>48 m; >400 m/s).

Unit 1 (as per the STA 133+58 boring log) corresponds with a zone comprised mostly of moderately stiff to stiff clay with some sand layers (~0-6 m); Unit 2 correlates with a zone comprised mostly of medium dense, gray sand with sparse gravel (~6-9 m); and Unit 3 and top of Unit 4 correlates with a zone comprised of mostly dense to very dense, medium to coarse grained sand with some light gravel (~9 m to base of log at ~20 m). Unit 5 was not tested at the L-302 Bridge location, however the general trend of the SASW shear-wave velocity curve compares favorably with data acquired at the A-3709 and A-5648 bridge Sites (Figures 6 and 8). At these locations, higher shear-wave velocities at progressively greater depths were associated with increasingly compacted sediment (predominantly sands). These SASW data and lithologic log data indicate there is a direct correlation between SASW shear-wave velocities and subsurface lithologies.

The L-302 XCPT seismic shear-wave velocity profile (Figure 15) does not appear to correlate as well with the subsurface lithology as determined at the corresponding STA 135+85 location. More specifically, Unit 1 (moderately stiff to stiff clay at depths of ~0-3 m) is characterized by shear-wave velocities ranging from ~70-75 m/s, while Unit 2 (medium- to coarse-grained, loose to dense sand at depths of ~3 m to base of borehole at ~9 m) is characterized by velocities ranging from ~95-295 m/s. (Moreover, the higher shear-wave velocities correspond to shallower depths.) Note that the XCPT curve and the OLD (1995-vintage SCPT) shear-wave velocity profiles differ appreciably.

A-5460 Bridge Site #6: The SASW-generated vertical shear-wave profile from the A-5460 Bridge Site (near STA 180) is shown as Figure 16. On the basis of average estimated interval shear-wave velocity, the SASW profile can be divided into five units: Unit 1 (~0-12 m; ~140-160 m/s); Unit 2 (~12-17 m; ~190-240 m/s); Unit 3 (~17-43 m; ~270-290 m/s); Unit 4 (~43-54 m; ~340-450 m/s); and Unit 5 (>54 m; >590 m/s).

Unit 1 (as per the STA 180+33 boring log) corresponds with a zone comprised mostly of sandy clay to clayey sand (~0-9 m), while Unit 2 correlates with a zone comprised mostly of dense to very dense, fine to medium grained sand (~9 m to base of borehole at ~17 m). Units 3, 4 and 5 were not tested at the STA 180+33 location, however the general trend of the SASW shear-wave velocity curve compares favorably with data acquired at the A-3709 and A-5648 bridge Sites (Figures 6 and 8). At these locations, higher shear-wave velocities at progressively greater depths were associated with increasingly compacted sediment (predominantly sands). These SASW data and lithologic log data indicate there is a direct correlation between SASW shear-wave velocities and subsurface lithologies.

The A-5460 XCPT seismic shear-wave velocity profile (Figure 18) does not appear to correlate very well with the lithologic units encountered at the STA 177+29 test site. More specifically, Unit 1 is (~0 m to base of borehole at ~10 m) is characterized by velocities ranging from ~120 m/s to ~240 m/s. Note also that the XCPT curve and the OLD (1995-vintage SCPT) shear-wave velocity profiles differ appreciably.

11. COMPARISON OF SASW AND SCPT VERTICAL SHEAR-WAVE PROFILES

The vertical SASW shear-wave velocity profiles presented herein, appear to correlate quite well with available subsurface lithologic control, cross-borehole shear-wave velocity control and depth of burial. For example, surficial clays, described as silty, are characterized by shear-wave velocities ranging from ~90 m/s to 140 m/s. Clays described as containing sand are characterized by velocities ranging from ~120 m/s to ~170 m/s. Clayey silts to silty sands are characterized by velocities ranging from ~130 m/s to ~230 m/s, with sediments described as stiffer exhibiting characteristically higher velocities.

The SASW shear-wave velocities of sediments described as sand vary significantly at each study site, however there appears to be a very definite pattern to the observed velocity variations. More specifically, the velocities of sand increase almost monotonically (in a step-wise manner) with depth at each test site, suggesting that the shear-wave velocities of these unconsolidated sands are a function of depth of burial. In terms of sands with similar depths of burial, those described as dense to very dense exhibit relatively higher SASW shear-wave velocities. The SASW shear-wave velocity profiles at Bridge site A-5648 (Site #2) correlates very well with available cross-borehole shear-wave control. More specifically, the subsurface sands (~6 m to ~48 m depth) are characterized by an SASW shear-wave velocity profile that increases step-wise (almost monotonically) from about 230 m/s to about 350 m/s. The cross-borehole shear-wave velocity profile (over the same depth interval) is characterized by velocities that increase gradually from ~245 m/s to ~380 m/s. The SASW shear-wave velocity profile at Bridge site A-1466 (Site #4) also correlates well with available cross-borehole shear-wave control.

The SCPT shear-wave velocities do not correlate nearly so well with subsurface lithologies. More specifically, surficial clays, described as silty, are characterized by shear-wave interval velocities ranging from ~45 m/s to ~145 m/s. Clays described as containing sand are characterized by interval velocities ranging from ~70 m/s to ~240 m/s. Clayey silts to silty sands are characterized by interval velocities ranging from ~90 m/s to ~300 m/s. Moreover, SCPT shear-wave velocities can vary significantly (>300%) within essentially the same lithologic unit over distances of only a few feet.

The geotechnical data presented herein indicate that the SASW shear-wave velocity profiles correlate well with subsurface lithologic logs and available cross-borehole shear-wave velocity control. More

specifically, clays, silts and sands are characterized by relatively characteristic SASW-velocities, which increase almost monotonically (step-wise and incrementally) with increasing depth of burial. We believe this study demonstrates that SASW shear-wave velocities are reliable.

The data presented herein also indicate that the SASW shear-wave profiles and borehole lithologic data do not correlate particularly well with the SCPT shear-wave velocity profiles (SCPT data) – particularly at shallow depths of investigation. In our opinion, the significant velocity variations that characterize the SCPT shear-wave velocity profiles are due mostly to the accuracy with which travel times can be measured over 1 m intervals. A visual examination of the shear-wave velocity profiles at each site, suggests the SCPT data would correlate more closely with CH and SASW velocity data if averaged over greater vertical distances.

On the basis of this study, we conclude that SASW shear-wave velocity profiles are reliable. In our opinion, the SASW technique can be used to estimate the engineering properties of soil.

12. CONCLUSIONS AND RECOMMENDATIONS

On the basis of this study, we conclude that SASW shear-wave velocity profiles are reliable. In our opinion, the SASW technique can be used to estimate the engineering properties of soil.

We recommend an expanded SASW study in an effort to further evaluate the strengths and weaknesses of the SASW tool. We recommend the acquisition of SASW, SCPT, cross-borehole and SPT data at multiple additional sites in Missouri in an effort to determine inter-relationships in a statistically meaningful way. We also recommend the acquisition of SASW data at select sites in Missouri, in an effort to assess the utility of this tool in terms of determining depth to bedrock, estimating the engineering properties of bedrock, and identifying heterogeneities (e.g. karstic cavities) within bedrock. Further, we recommend the acquisition of SASW data across paved roadways in order to assess the capabilities of this tool in terms of estimating asphalt and pavement thicknesses, and sub-grade conditions.

13. SUGGESTED REFERENCES

Aki, K., and Richards, P.G., 1980, *Quantitative Seismology*: W.H.Freeman & Co., San Francisco, 932 p.

Bullen, K.E., 1963, *An Introduction to the Theory of Seismology*: Cambridge University Press, 381 p.

Herrmann, R.B., 1996, *Computer Programs in Seismology*: Saint Louis University Press, Saint Louis, Missouri.

Liu, H.P., Boore, D.M., Joyner, W.B., Oppenheimer, D.H., Warrick, R.E., Zhang, W., Hamilton, J.C., and Brown, L.T., 2000, Comparison of phase velocities from array measurements of Rayleigh waves associated with micro-tremor and results calculated from borehole shear-wave velocity profiles: *Bulletin Seismological Society of America*, **90**, 666-678.

Kramer, S.L., 1996, *Geotechnical Earthquake Engineering*: Prentice-Hall Inc., 653 p.

Miller, R.D., Xia, J., Park, C.B., and Ivanov, J., 2000, Shear-wave velocity field from surface waves to detect anomalies in the subsurface: *Geophysics 2000*, FHWA and MoDOT Special Publication, 4:8.1–4:8.10.

Nazarian, S., Stokoe, K.H., and Hudson, W.R., 1983, Use of spectral analysis of surface waves method for determination of moduli and thicknesses of pavement systems: *Transportation Research Record*, **930**, 38-45.

Park, C.B., Miller, R.D., and Xia, J., 1999, Multichannel analysis of surface waves: *Geophysics*, **64**, 800-808.

Park C.B., Miller, R.D., and Xia J., 1999, Multimodal analysis of high frequency surface waves: *Proceeding of the Symposium on the Application of Geophysics to Engineering and Environmental Problems*, 115-121.

Park, C.B., Miller, R.D., Xia, J., and Ivanov, J., 2000, Multichannel seismic surface-wave methods for geotechnical applications: *Geophysics 2000*, FHWA and MoDOT Special Publication, 4:7.1-4:7.11.

Press W.H., Teukolsky, S.A., Vetterling, W.T., and Flannery, B.P., 1997, *Numerical Recipes in C: The Art of Scientific Computing*: Cambridge University Press, 965 p.

Rechtien, D., 2002, *Inversion of Liquefaction Relevant Seismic Data*: U.S. Army Corps of Engineers Contract Report GL-02-1, 64 p.

Stokoe, K.H., Wright, G.W., James, A.B., and Jose, M.R., 1994, Characterization of geotechnical sites by SASW method, *in Geophysical Characterization of Sites ISSMFE Technical Committee #10*, edited by R.D. Woods: Oxford Publishers, New Delhi

Xia, J., Miller, R.D., and Park, C.B., 1999, Estimation of near-surface velocity by inversion of Rayleigh waves: *Geophysics*, **64**, 691-700.

Zywicki, D.J., and Rix, G.J., 1999, Frequency-wavenumber analysis of passive surface waves: *Proceeding of the Symposium on the Application of Geophysics to Engineering and Environmental Problems*, 75-84.

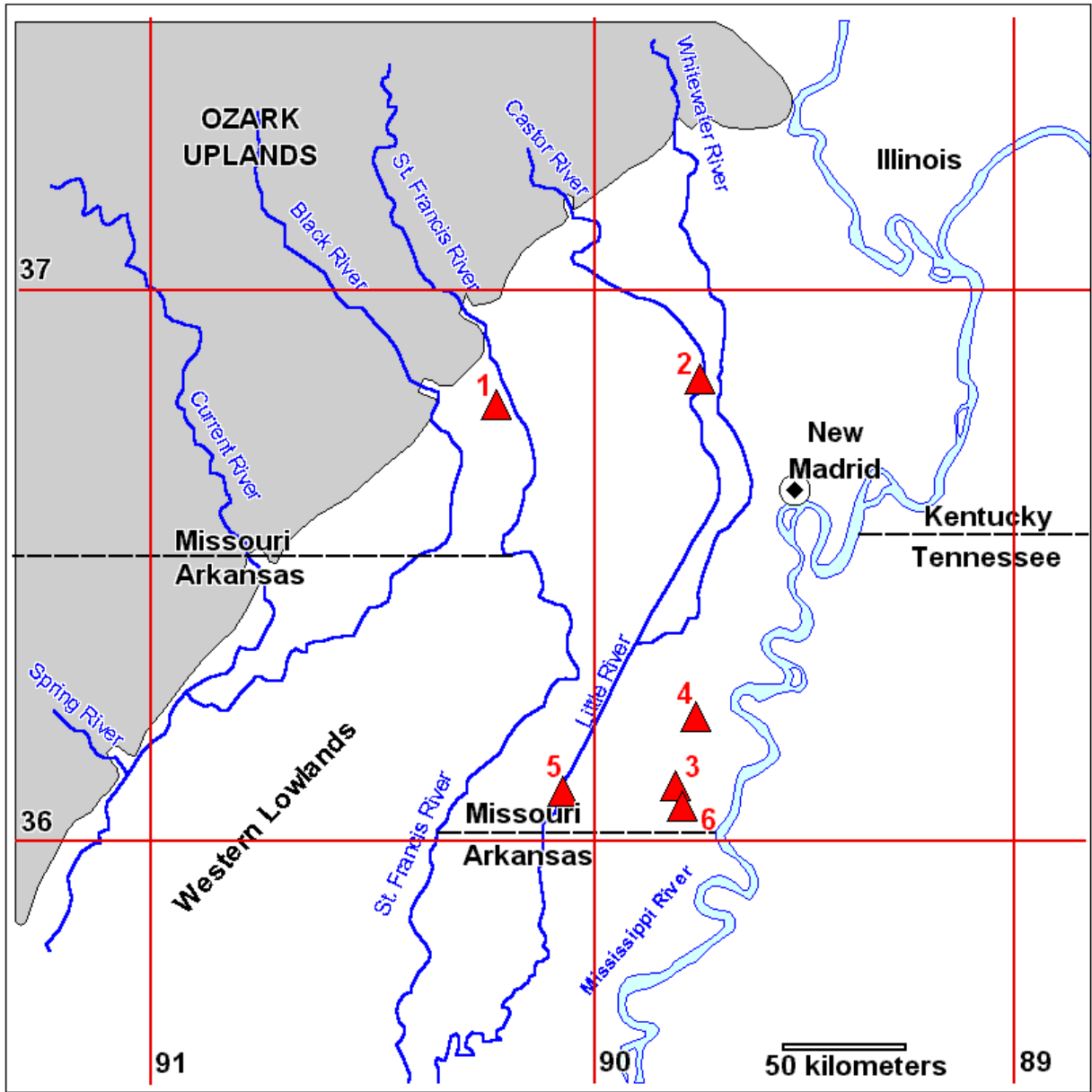


Figure 4: Map of Southeast Missouri showing locations of SASW test sites. Δ denotes SASW test site. (Site #1: A-3709 Bridge; Site #2: A-5648 Bridge; Site #3: L-472 Bridge; Site #4: A-1466 Bridge; Site #5: L-302 Bridge; Site #6: A-5460 Bridge.)

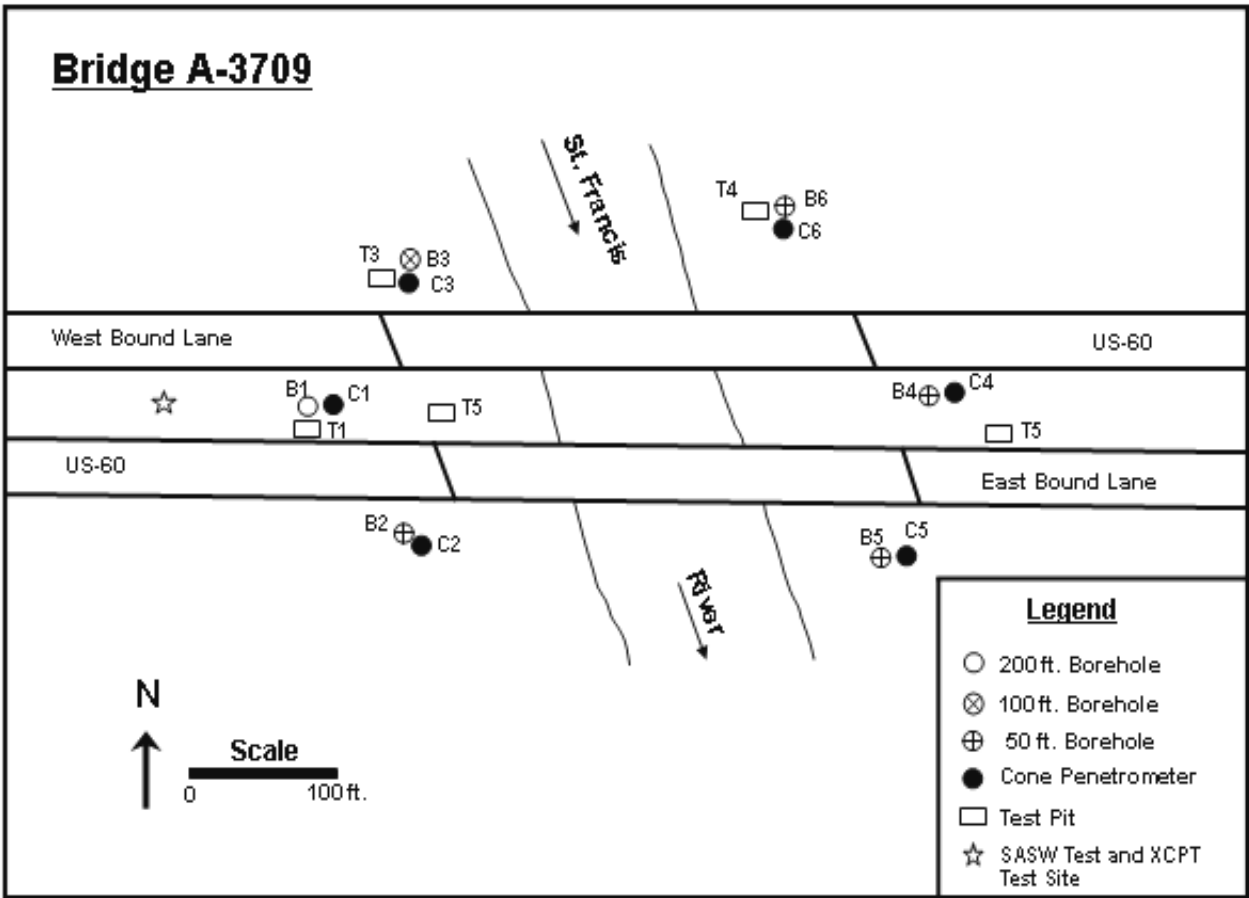


Figure 5: A-3709 Bridge Site #1 (Figure 4).

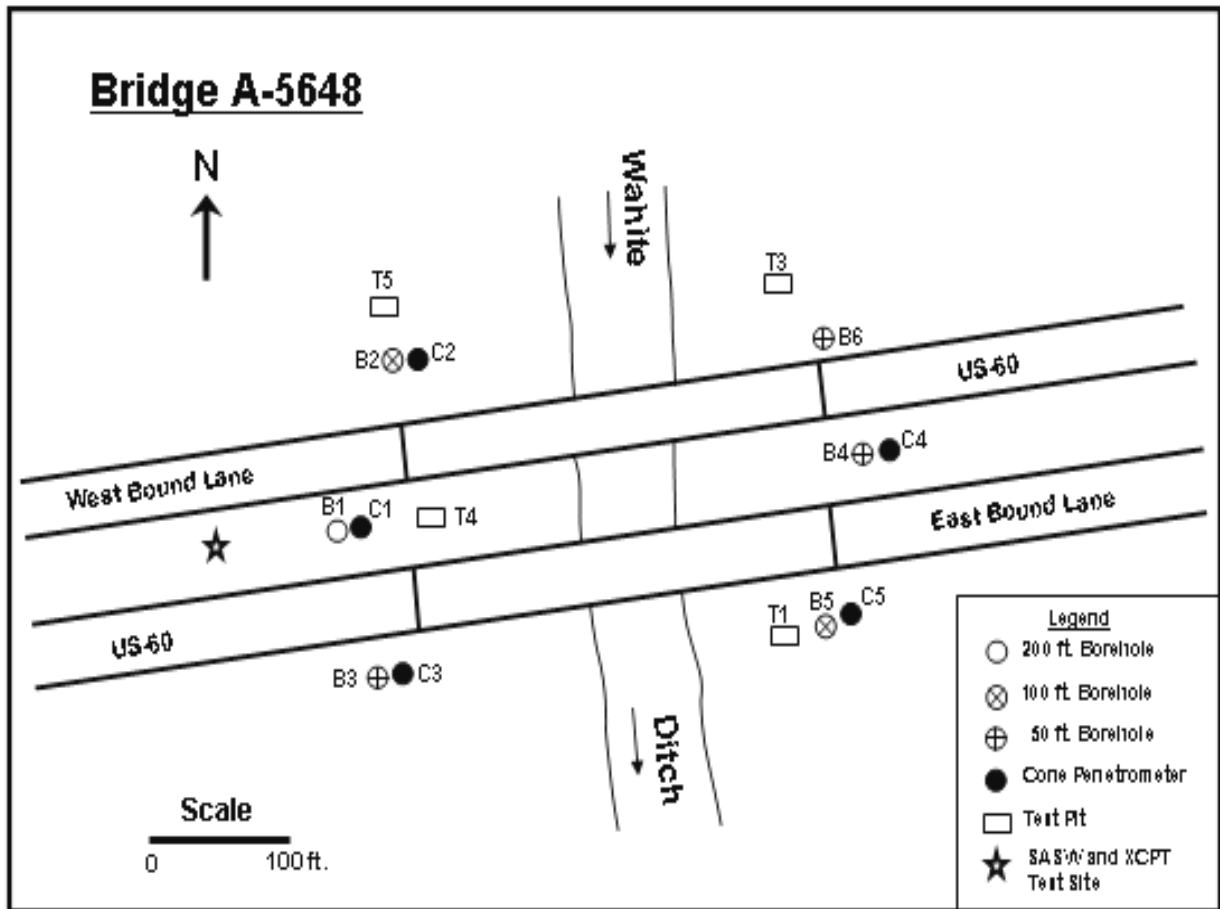


Figure 6: A-5648 Bridge Site #2 (Figure 4).

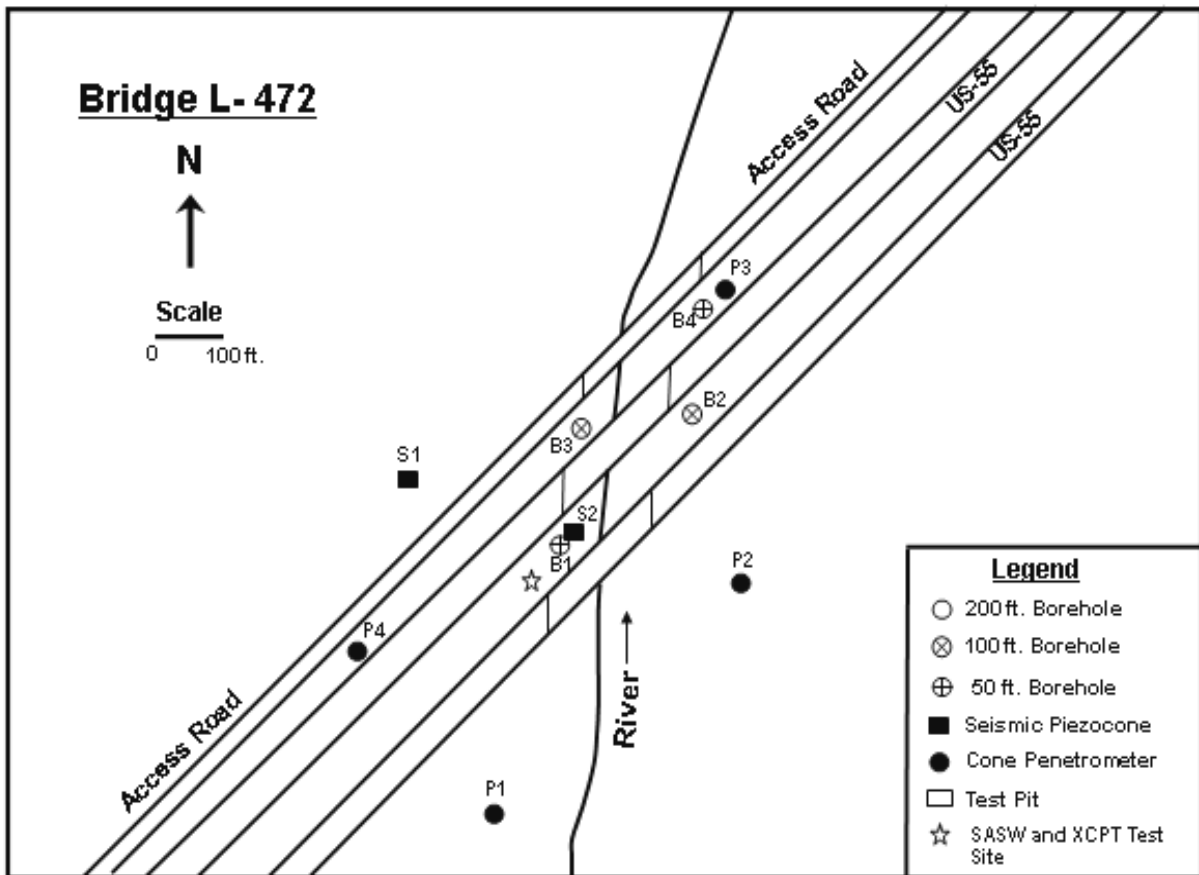


Figure 7: L-472 Bridge Site #3 (Figure 4).

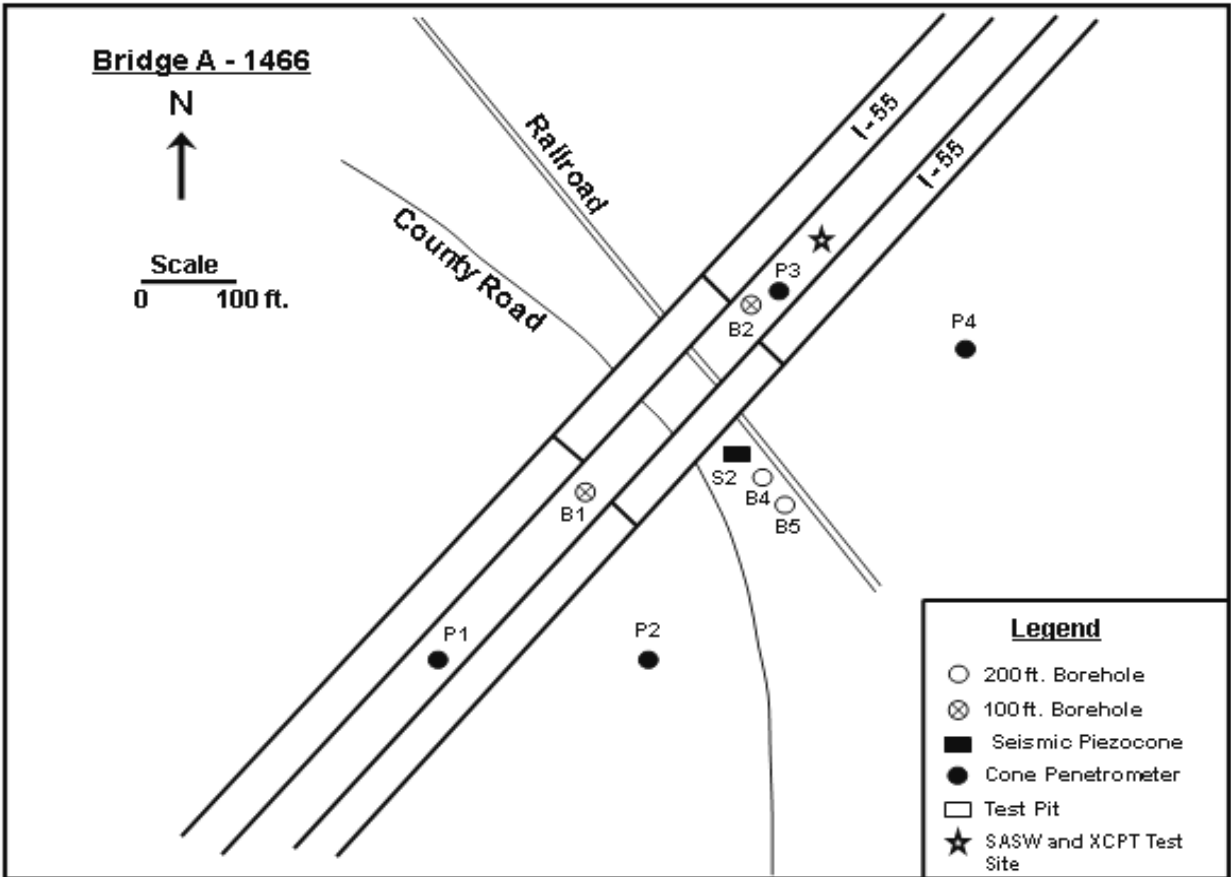


Figure 8: A-1466 Bridge Site #4 (Figure 4).

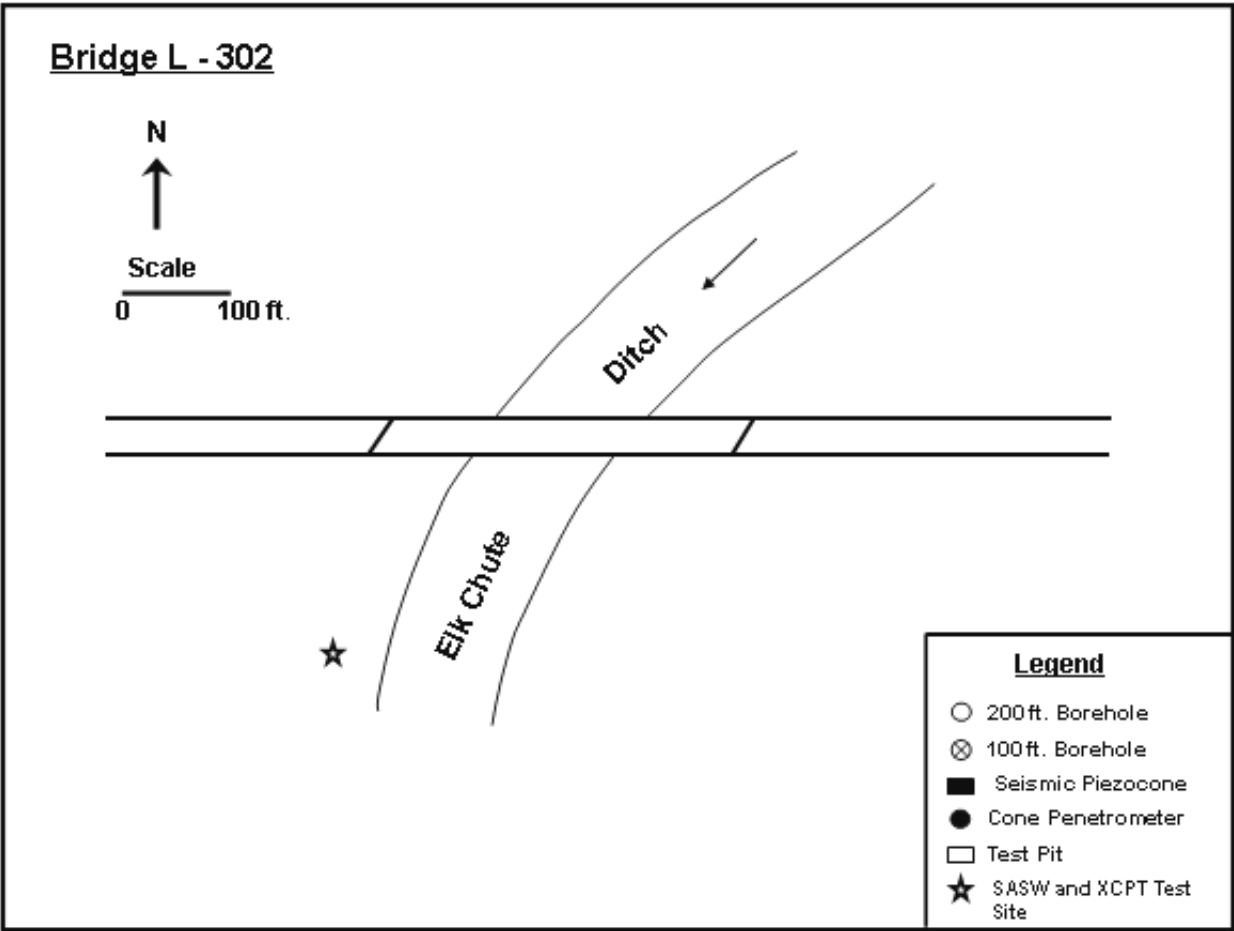


Figure 9: L-302 Bridge Site #5 (Figure 4).

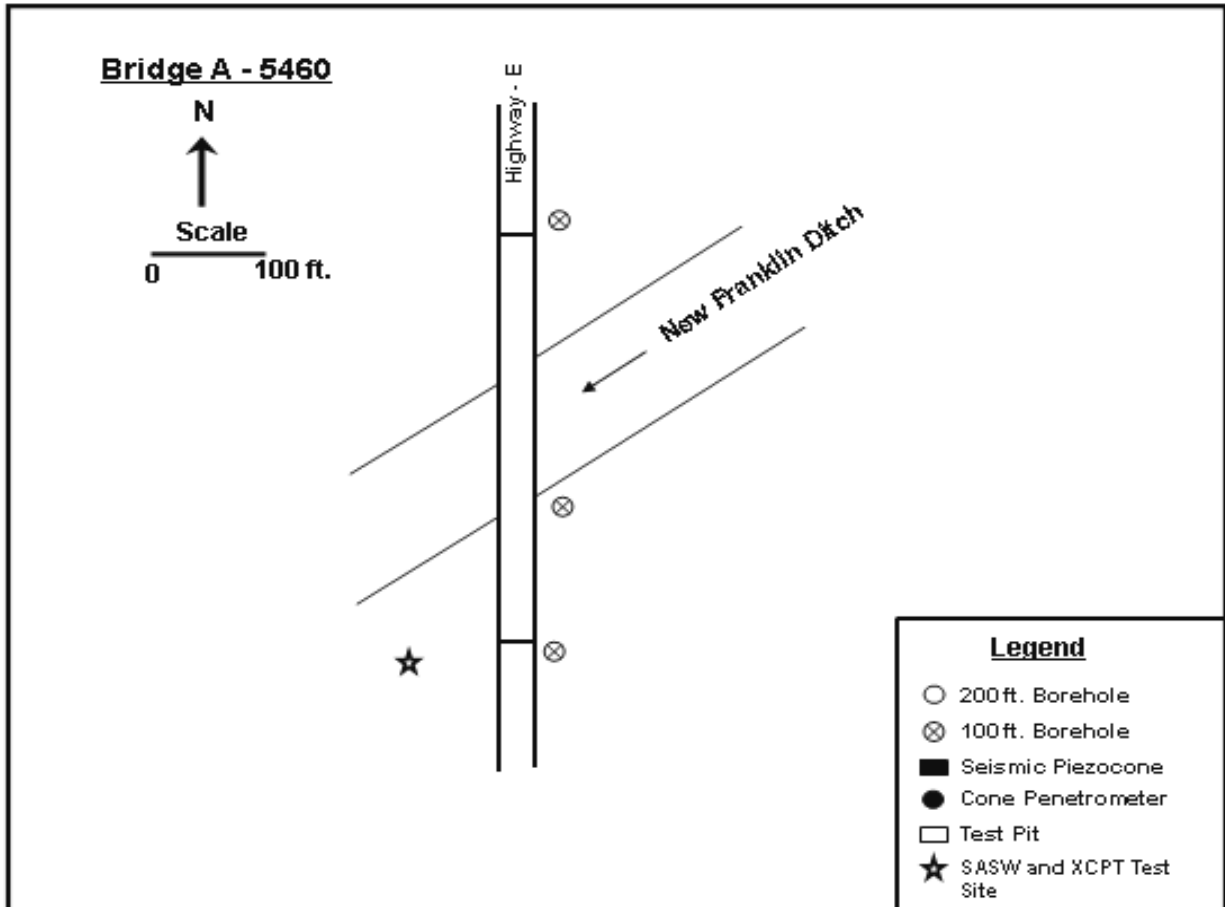


Figure 10: A-5460 Bridge Site #6 (Figure 4).

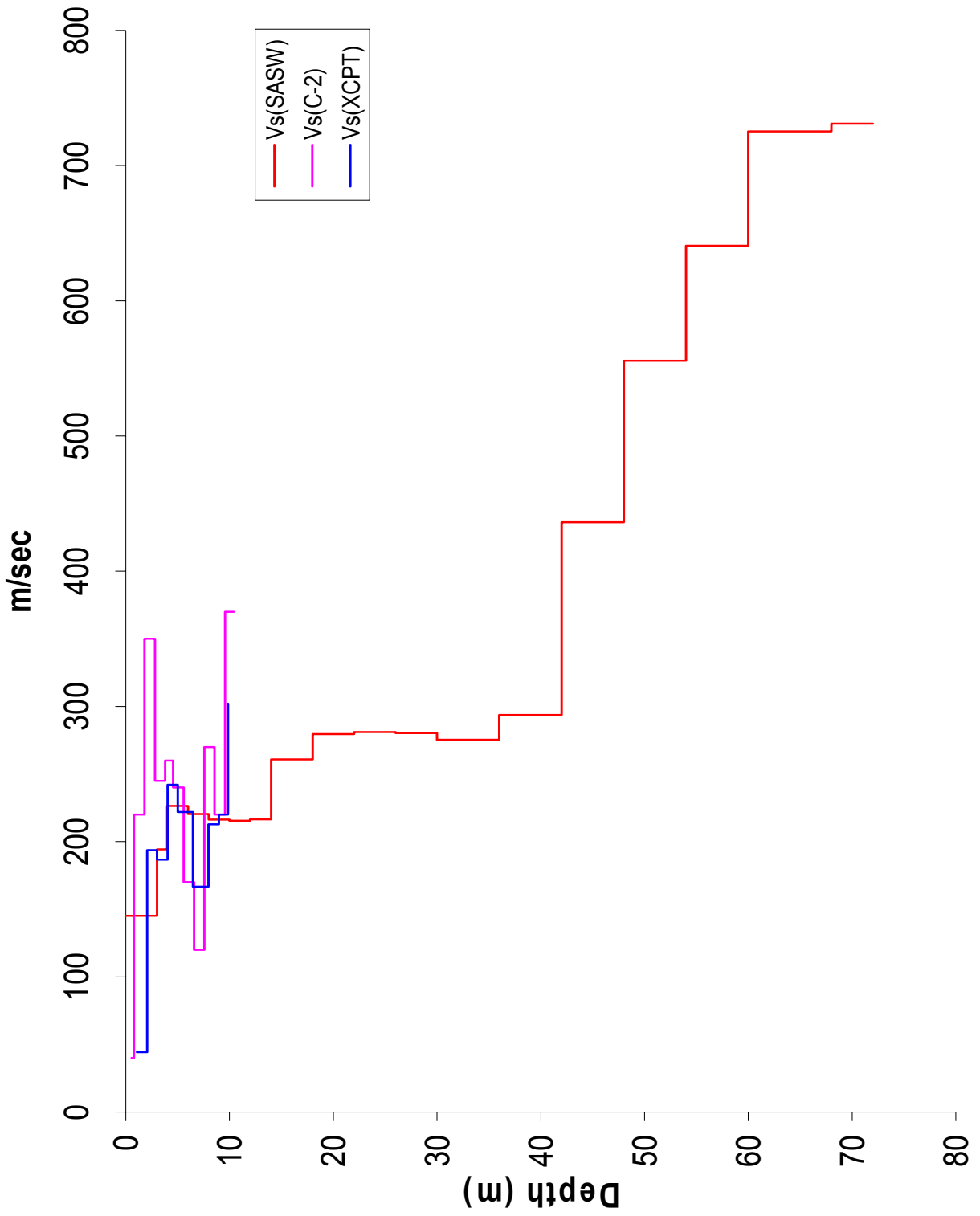


Figure 11: Shear-wave velocity profiles for A-3709 Bridge Site#1 (Figure 4 and 5).

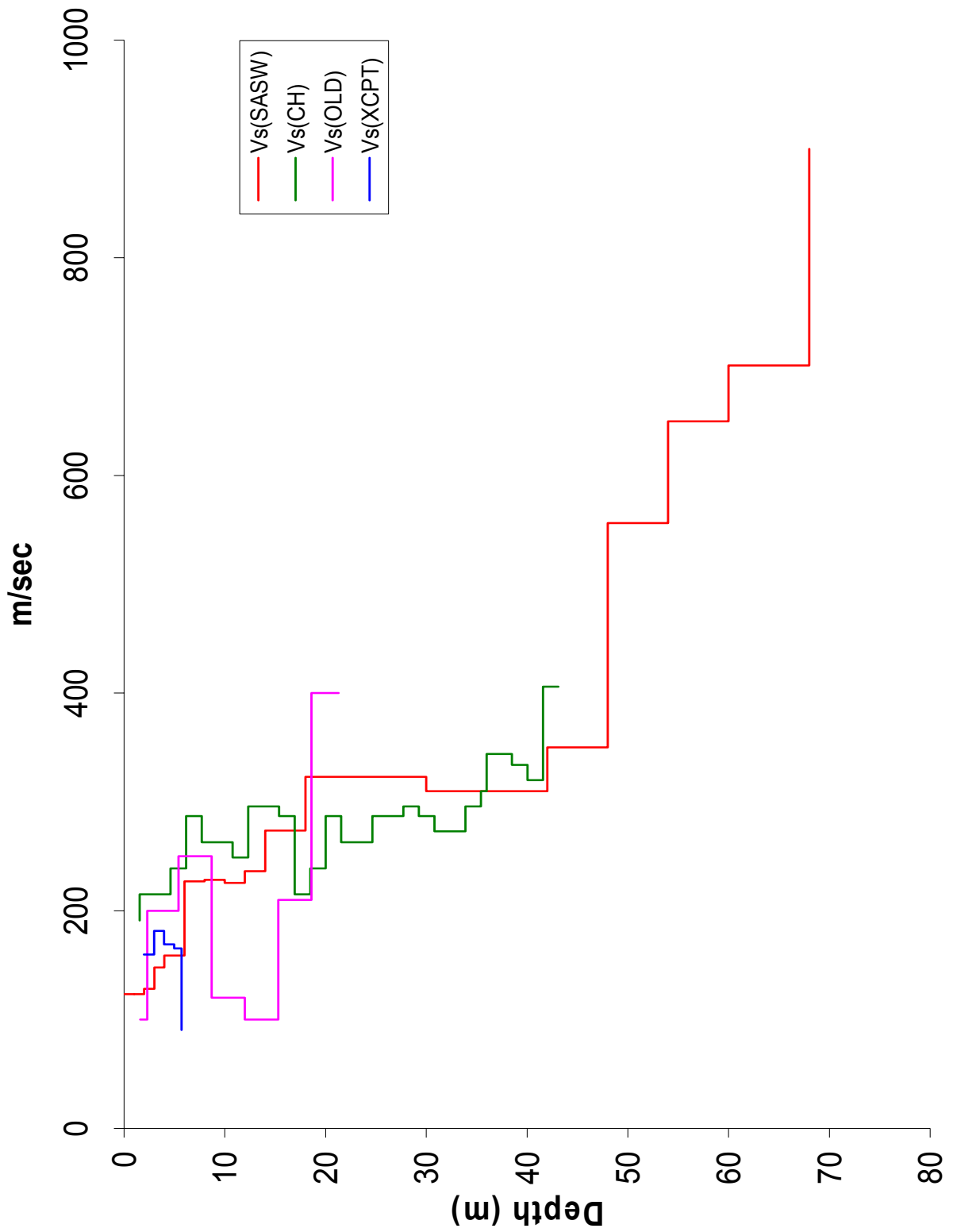


Figure 12: Shear-wave velocity profiles for A-5648 Bridge Site#2 (Figure 4 and 6).

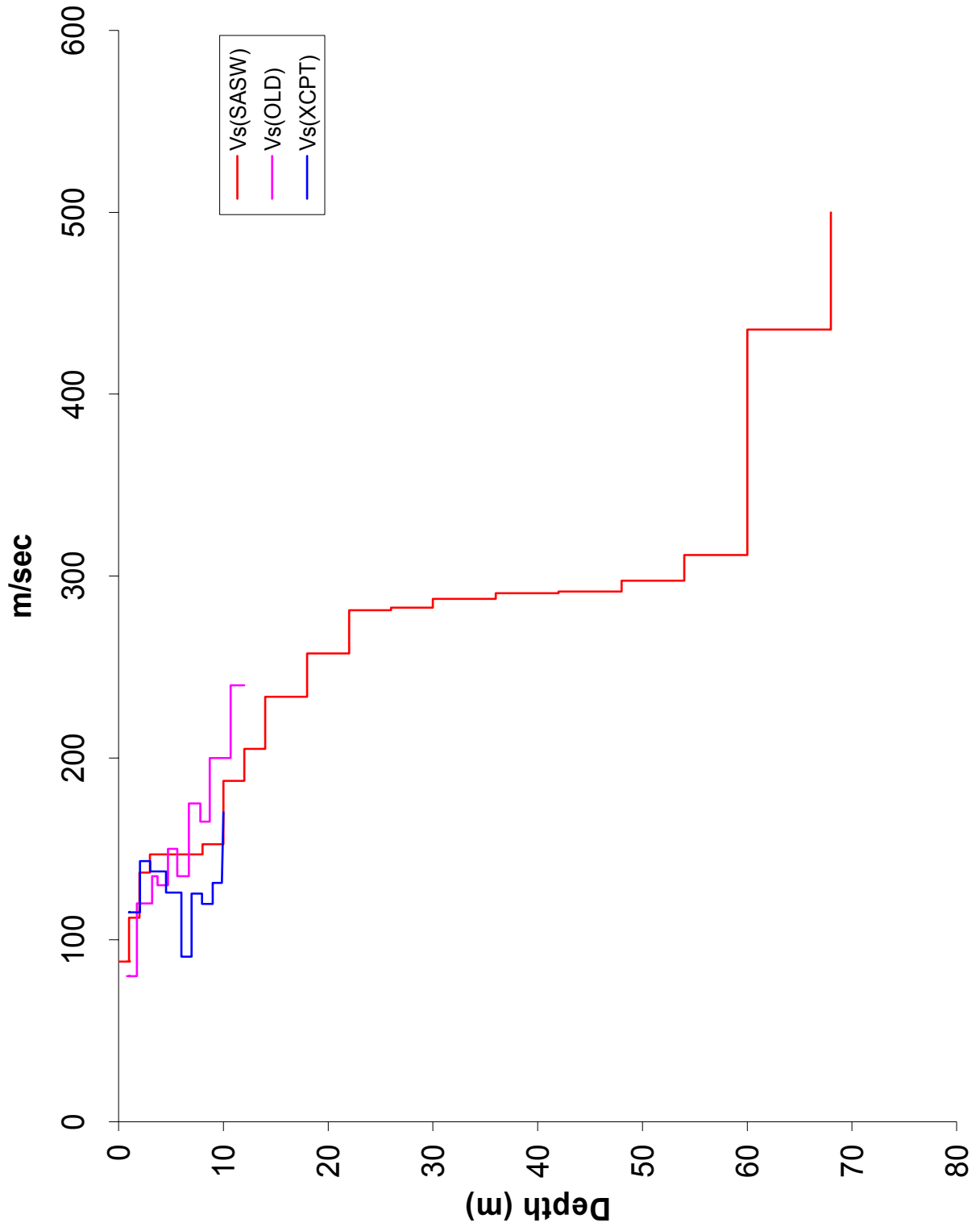


Figure 13: Shear-wave velocity profiles for L-472 Bridge Site#3 (Figure 4 and 7).

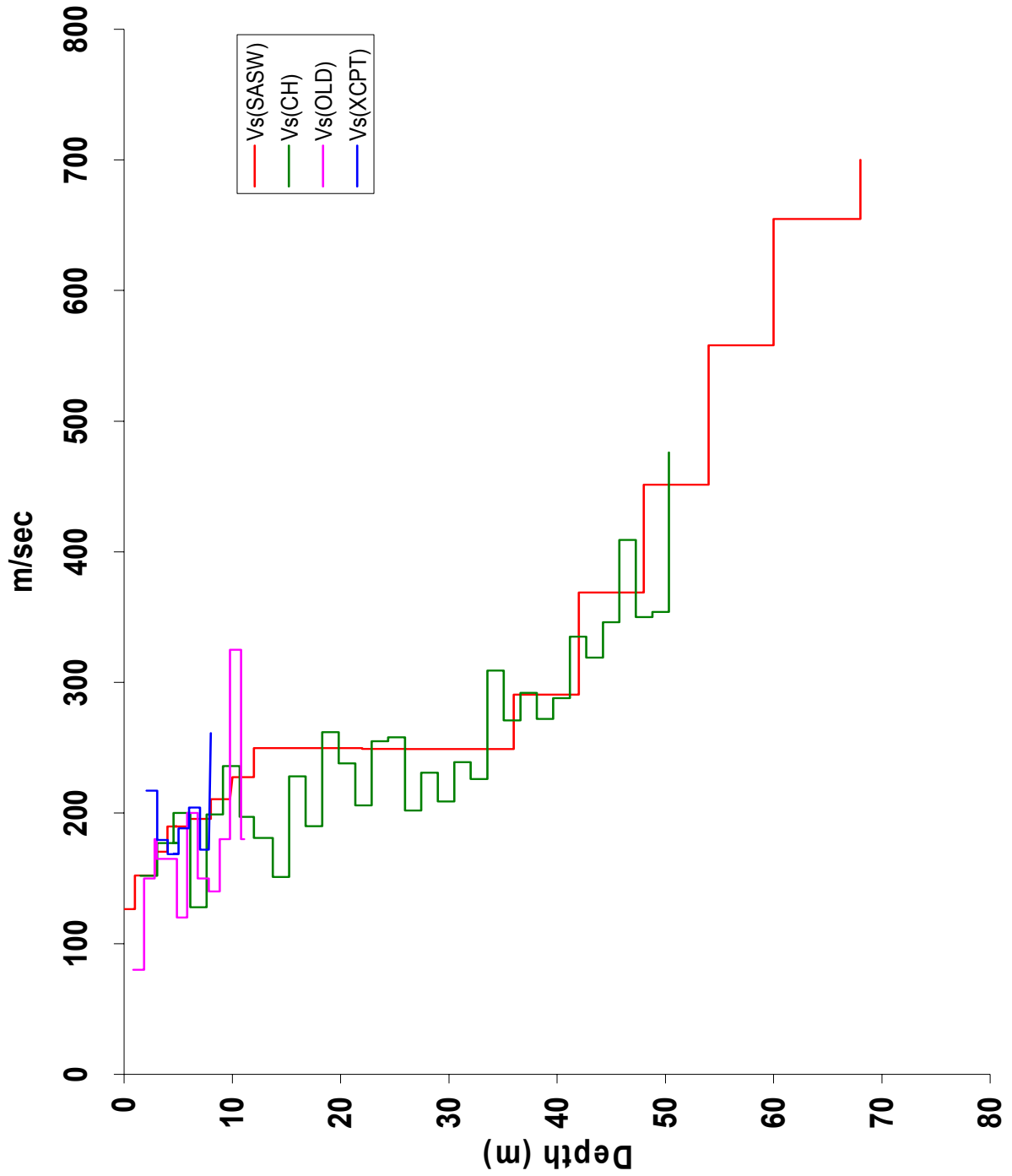


Figure 14: Shear-wave velocity profiles for A-1446 Bridge Site#4 (Figure 4 and 8).

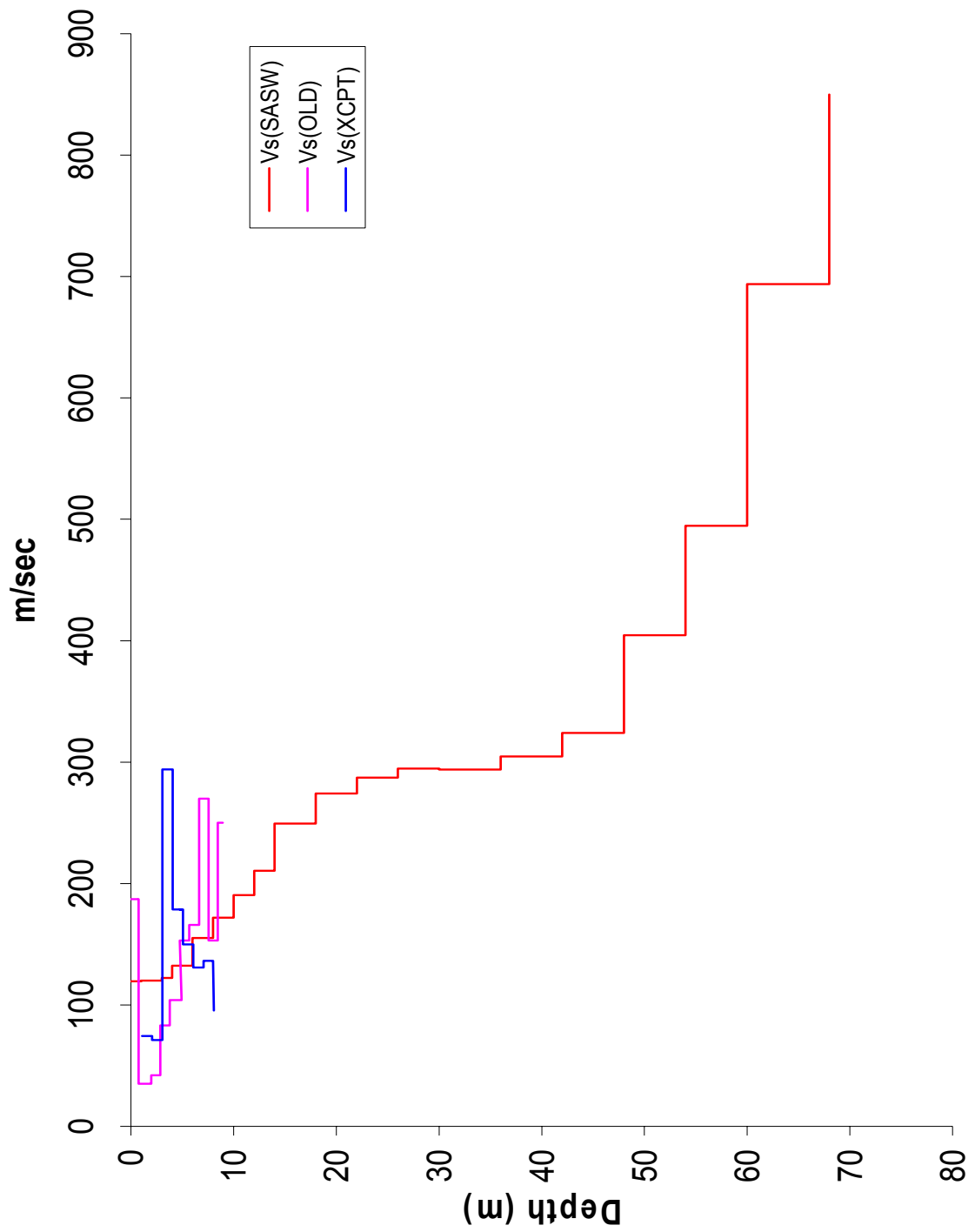


Figure 15: Shear-wave velocity profiles for L-302 Bridge Site#5 (Figure 4 and 9).

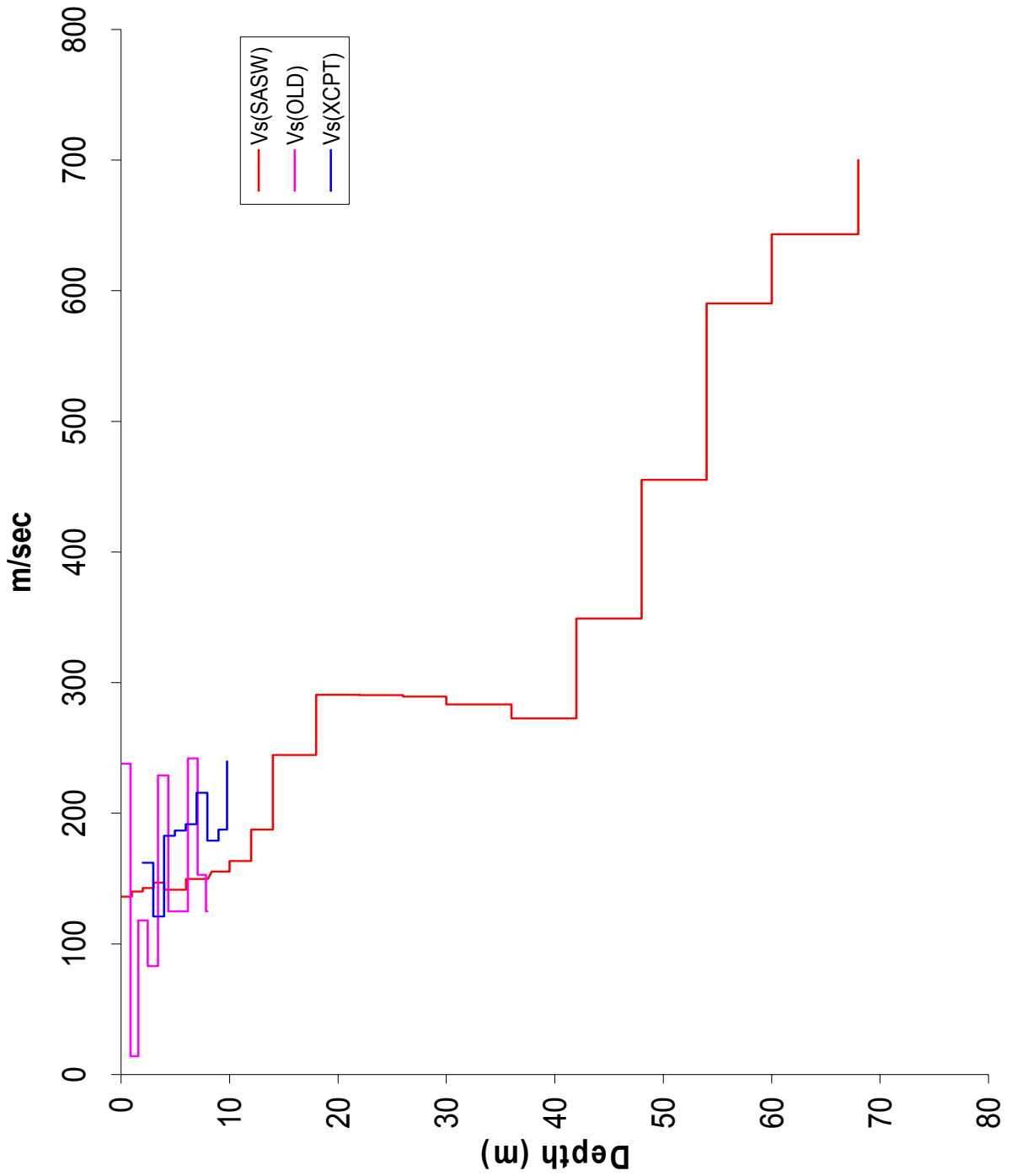


Figure 16: Shear-wave velocity profiles for A-5460 Bridge Site#6 (Figure 4 and 10).